Time-domain ferromagnetic resonance in epitaxial thin films

D. M. Engebretson, J. Berezovsky,[a] and J. P. Park
School of Physics and Astronomy, University of Minnesota, Minneapolis, Minnesota 55455

L. C. Chen and C. J. Palmstrøm
Department of Chemical Engineering and Materials Science, University of Minnesota, Minneapolis, Minnesota 55455

P. A. Crowell
School of Physics and Astronomy, University of Minnesota, Minneapolis, Minnesota 55455

Time-resolved ferromagnetic resonance is used to study magnetic relaxation in epitaxial $Fe_{1-x}Co_x$ films grown on vicinal GaAs(100) surfaces. The magnetic free energy of these films is determined by a combination of a four-fold volume anisotropy and a two-fold anisotropy due to surface bonding and morphology. The response following a high bandwidth (~10 GHz) magnetic field pulse is measured using the polar Kerr effect. Samples with transverse dimensions much larger than the spatial extent of the field pulse show simple free induction decays. The measured precession frequencies are in good agreement with a coherent rotation model in the case of films grown on (100) surfaces with little or no (<2°) miscut. The magnetic response of 20 μm diameter disks is more complicated, particularly for static fields along the hard direction. Long-lived features appear in the response, and single precession frequencies are no longer observed. Micromagnetic simulations indicate the critical role played by the combination of the anisotropy and demagnetizing fields in the patterned structures. © *2002 American Institute of Physics.*
[DOI: 10.1063/1.1450817]

Ferromagnetic multilayers are a familiar component of storage technologies and an important model system for our understanding of fundamental magnetism. Although all-metallic systems such as Co–Cu are most familiar to physicists and engineers, heterostructures of ferromagnetic metals and semiconductors have been the focus of considerable recent work on spin transport and dynamics. Many of these experiments have focused on the important problem of spin injection,[1,2] but the ferromagnet–semiconductor system also provides an excellent opportunity for the study of spin dynamics in ferromagnets. Films of high crystalline quality can be grown by molecular-beam epitaxy, and the magnetic anisotropy can be tuned by modifying the morphology and bonding at the ferromagnet–semiconductor interface.[3–5] An important question that can be addressed by these systems is the role of the interface in determining the characteristic decay mode and damping of magnetic excitations.

We have used time-resolved ferromagnetic resonance to study the magnetization dynamics of epitaxial $Fe_{1-x}Co_x$ ($x \sim 0.5$) films grown on (2×4)-reconstructed GaAs (100) surfaces. Details of the growth procedure,[6] as well as the basic magnetic properties[5] of these films, have been reported previously. Three samples are discussed here. One was grown on the flat (100) surface, while the other two were grown on surfaces miscut by 2° and 8° towards a (111)A surface. The miscut results in steps running along the [011] direction and enhances the uniaxial anisotropy already present due to the two-fold symmetry of the reconstructed surface. For films of the thicknesses (<200 Å) under discussion here, the magnitude of the effective uniaxial anisotropy is larger than the intrinsic four-fold magnetocrystalline anisotropy. This leads to a distinct reversal mechanism when a magnetic field is applied along the [011] axis, in which a first-order transition occurs at a nonzero *split field* H_s as the applied field is reduced from saturation. Depending on the relative magnitudes of the uniaxial and magnetocrystalline anisotropies, as well as the surface terrace length, the transition at the split field can occur by either coherent rotation (towards [011]) or domain nucleation.[7] Hysteresis loops for fields along [011] are shown in Fig. 1 for each of the samples in this study. (The loops for fields along [011] and [010] show conventional easy and intermediate axis behavior.) In the case of the flat and 2° miscut samples, the discontinuity at H_s is a nearly 90° coherent rotation towards [011] as determined by magneto-optical Kerr effect (MOKE) and vibrating sample magnetometer (VSM) measurements at different field orientations.[6] The 8° miscut sample shows nucleation behavior near the split field.[8]

Pulsed ferromagnetic resonance allows for a complete mapping of the free-energy surface of these films while si-

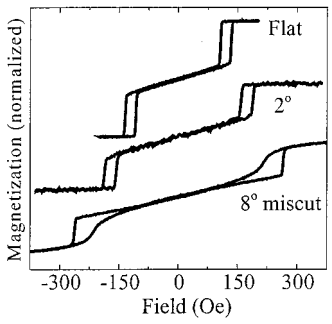

FIG. 1. Hysteresis loops measured along $[01\bar{1}]$ for the three samples of this study. Note that the jump in the magnetization at the split field occurs directly from the fully magnetized state in the flat and 2° miscut samples.

[a]Electronic mail: crowell@physics.umn.edu

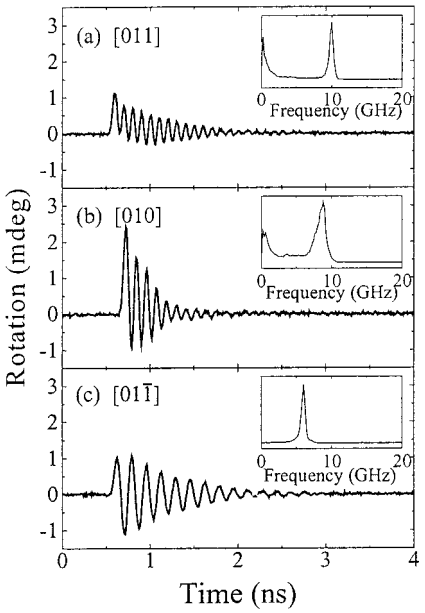

FIG. 2. Time-domain data obtained for a film of epitaxial $Fe_{0.5}Co_{0.5}$ on GaAs(100) without miscut. An in-plane field of 200 Oe is applied along each of the three principal directions: (a) [011], the magnetic easy axis of the sample, (b) along [010], and (c) along [011], the magnetic hard axis. Fourier transforms of the time-domain data are shown in the insets.

multaneously providing a direct time-domain probe of magnetic relaxation. The technique has been used by several groups[9–11] to study relaxation processes in polycrystalline films. In our approach, a free-standing sample, with the substrate polished to a thickness of 25 μm or less, is placed on a 30 μm wide section of a microstrip transmission line. The sample can be rotated about the polar axis, allowing for any orientation of the microwave and static fields relative to the in-plane crystalline axes. An 8 mm taper on each side connects the narrow section to standard 50 Ω lines. A current pulse is discharged into the stripline from a fast photodiode (rise time ~60 ps) triggered by a Ti:Sapphire laser. The z component of the magnetization is probed by measuring the polar Kerr rotation of a time-delayed probe pulse with a polarization bridge referenced to the pump chopping frequency.

Time traces for an unpatterned flat $Fe_{0.5}Co_{0.5}$/GaAs (100) sample are shown in Fig. 2 for a field of 200 Oe applied along the [011], [010], and [011] directions. The sample dimensions of order 1–2 mm are much larger than the stripline width. Fourier transforms of the time-domain signals are shown in the insets of Fig. 2. Unlike for the other two directions, the magnetization along [010] is not saturated at 200 Oe. This may be the origin of the shorter relaxation time (and larger linewidth) observed in Fig. 2(b).

A more complete picture of the dynamics is given in Fig. 3, which shows the FMR frequencies determined from the Fourier transforms of the time-domain data for fields along the three principal directions in each sample. The solid curves in Fig. 3 show fits to the FMR frequencies in the effective field model,[12] in which

$$\omega = \gamma H_{\text{eff}} = \frac{\gamma}{M \sin\theta}\left\{\frac{\partial^2 F}{\partial\theta^2}\frac{\partial^2 F}{\partial\varphi^2} - \left(\frac{\partial^2 F}{\partial\theta\partial\varphi}\right)^2\right\}^{1/2}, \quad (1)$$

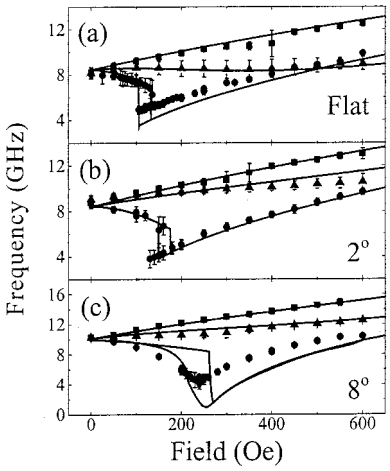

FIG. 3. The precession frequency is shown as a function of magnetic field for the three principal field orientations: [011] (squares), [010] (triangles), and [011] (circles). Data are shown for three samples: (a) $Fe_{0.5}Co_{0.5}$ grown on flat GaAs(100), (b) miscut 2° towards (111)A, and (c) miscut 8° towards (111)A. The solid curves represent fits to the model discussed in the text.

and the free-energy F is

$$F = -\mathbf{M}\cdot\mathbf{H} + \frac{K_\nu}{4}(\sin^2 2\theta + \sin^2 2\varphi \sin^4\theta) + K_u \sin^2\theta \cos^2\left(\varphi - \frac{\pi}{4}\right) + (2\pi M^2 + K_\perp)\cos^2\theta, \quad (2)$$

where M is the magnetization, θ and φ are the polar and azimuthal angles measured from [100] and [010] respectively, K_ν is the four-fold anisotropy, K_u is the in-plane uniaxial anisotropy, and $K_\perp$ is a perpendicular anisotropy constant. In practice, $K_\perp$ is the only fitting parameter for the FMR data and is determined by a least squares fit of the easy and intermediate axis frequencies as a function of field. The magnetization and all of the in-plane anisotropy constants were determined from VSM measurements and fits to a simple coherent rotation model. The magnetization data were also used to determine the azimuthal angle φ at each field. Once the fitting of the data for the [011] and [010] directions was completed, the theoretical curves for the [011] direction were generated without any further adjustment of the parameters. While there is good qualitative agreement with the experiment in the flat and 2° samples, there are significant discrepancies in the case of the 8° miscut sample. This is not entirely surprising given the fact that the much stronger contribution to the anisotropy from step edges favors domain nucleation over coherent rotation as vicinality increases.[7] Interestingly, the damping in this sample near the split field is not significantly larger than in the less vicinal samples.

One great advantage of the time-domain technique is its potential for testing micromagnetic models of magnetization dynamics in small particles.[13] To obtain a more controlled geometry, we patterned samples into arrays of 20 μm diameter disks. The samples were positioned under a microscope so that one of the disks was centered over the stripline. Since the substrate thickness is approximately 25 μm, there is an approximately 6% variation in the magnitude of the pulsed field over the area of the sample. The probe beam was fo-

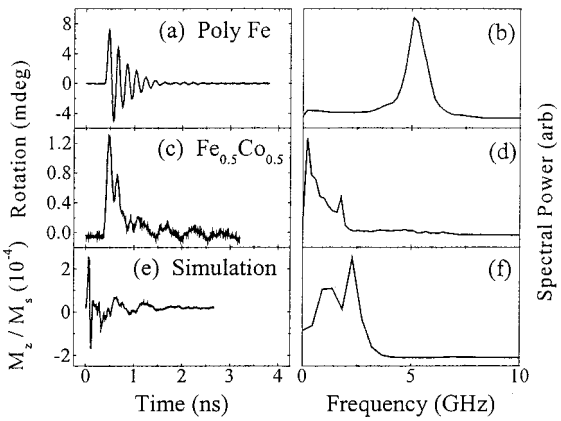

FIG. 4. Experimental data and simulations of the magnetic relaxation of disks in applied fields of 150 Oe along [011]. Time-domain data are shown in (a) for a 20 μm diameter disk of polycrystalline Fe with the associated Fourier transform shown in (b). Panels (c) and (d) show time-domain data and the fast Fourier transform (FFT) for a 20 μm diameter disk of $Fe_{0.5}Co_{0.5}$. Panels (e) and (f) show time-domain data and the FFT from a micromagnetic simulation of a 2 μm diameter $Fe_{0.5}Co_{0.5}$ disk.

cused to a spot with a diameter of approximately 5 μm. Patterned disks of polycrystalline Fe show a single well-defined precession frequency, as can be seen in Fig. 4(a), and the dependence on magnetic field (not shown) follows the canonical form expected for a thin film with only shape anisotropy. For disks of epitaxial $Fe_{1-x}Co_x$ on a flat (100) surface, the time-domain scans for fields along [011] and [010] show essentially the same precession frequencies as observed for the unpatterned films. However, the behavior of the disks is significantly different when the magnetic field is applied along the [011] direction. Figure 4(c) shows time-domain data and their Fourier transform for a field of 150 Oe. The low-frequency beating in this case persists at time scales beyond the decay times observed in unpatterned films. Even at higher fields, above the split field, we find considerable structure in the hard-axis free induction decays.

The data of Fig. 4(c) are an indication of a spatially inhomogeneous response to the field pulse. Although full-scale imaging is required to address this issue, some insight can be gained by micromagnetic simulations, which clearly show how the combination of the in-plane demagnetizing field and the magnetocrystalline anisotropy is responsible for the more complicated response observed in the disks. We use the object oriented micromagnetic framework (OOMMF) code developed at the National Institute of Standards and Technology (NIST)[14] to model the ferromagnetic disk as a two-dimensional grid of uniformly magnetized cells. The effective field is calculated in each cell, and the Landau–Lifshitz–Gilbert equation is integrated to find the change in the magnetization of each cell at each time step. The code was modified to include cubic and uniaxial anisotropies simultaneously.

The dimensions of the cells used in the simulation were 5 nm by 5 nm by 20 nm. The lateral cell size was chosen to be significantly less than the domain wall thickness ($\sim$30 nm), but we were then limited to modeling disks with a maximum diameter of 2 μm. Despite the difference in length scale, there is reasonably good qualitative agreement in the domain structure between simulations and images of the 20 μm $Fe_{0.5}Co_{0.5}$ disks made with magnetic force microscopy.[15]

Initial conditions for a time-domain simulation were obtained by starting from the fully magnetized state and relaxing in successively smaller fields until the desired starting field was reached. A Gaussian field pulse with an amplitude of 10 Oe and a full width at half maximum of 140 ps was then applied. Figure 4(e) shows M_z/M_S as a function of time integrated over the disk in an applied field of 150 Oe with a Gilbert damping parameter $\alpha = 0.01$. As at other fields in the split-field regime, the simulations show the long-lived features observed experimentally. There is a strong correlation between the existence of edge domains and the low-frequency beating. For example, turning off the in-plane component of the demagnetizing field in order to remove the edge domains restores a single-component response. The simulations also establish that the spatially inhomogeneous pulse in a large sample also produces only a single precession frequency.

Although movies of the simulations have been produced, we do not have a detailed understanding of the relaxation process in the presence of the realistic anisotropy and demagnetizing fields. One important observation from the simulations is that for a given set of anisotropy parameters and damping constant, the decay time for the envelope of the z component of the magnetization, integrated over the disk, is found to be up to 25% shorter for disks than for large samples, indicating substantial inhomogeneous dephasing. Spatial imaging will be required to address this issue experimentally.

The authors acknowledge C. E. Campbell for indispensable advice on the micromagnetic simulations and A. Lungu for performing magnetic force microscopy on the disk samples. This work was supported by the Research Corporation, NSF DMR-9983777, the Alfred P. Sloan Foundation, ONR Grant No. N/N00014-99-1-0233 for one of the authors (C.J.P.), and the University of Minnesota Supercomputing Institute.

[1] H. J. Zhu *et al.*, Phys. Rev. Lett. **87**, 016601 (2001).
[2] A. F. Isakovic *et al.*, Phys. Rev. B **64**, 161304R (2001).
[3] E. M. Kneedler *et al.*, Phys. Rev. B **56**, 8163 (1997).
[4] A. Filipe, A. Schuhl, and P. Galtier, Appl. Phys. Lett. **70**, 129 (1997).
[5] A. F. Iskaovic *et al.*, J. Appl. Phys. **89**, 6674 (2001).
[6] L. C. Chen *et al.*, J. Vac. Sci. Technol. B **18**, 2057 (2000).
[7] R. A. Hyman, A. Zangwill, and M. D. Stiles, Phys. Rev. B **58**, 9276 (1998).
[8] A. F. Isakovic *et al.* (unpublished).
[9] W. K. Hiebert, A. Stankiewicz, and M. R. Freeman, Phys. Rev. Lett. **79**, 1134 (1997).
[10] T. J. Silva, C. S. Lee, T. M. Crawford, and C. T. Rogers, J. Appl. Phys. **85**, 7849 (1999).
[11] Y. Acremann *et al.*, Science **290**, 492 (2000).
[12] G. V. Skrotskii and L. V. Kurbatov, in *Ferromagnetic Resonance*, edited by S. V. Vonsovskii (Pergamon, Oxford, 1966), p. 12.
[13] B. C. Choi *et al.*, Phys. Rev. Lett. **86**, 728 (2001).
[14] M. J. Donahue and D. G. Porter, *OOMMF User's Guide, Version 1.0*, in Interagency Report NISTIR 6376, National Institutes of Standard and Technology (1999).
[15] A. Lungu (unpublished).